Scientia Iranica D (2023) 30(1), 142–153

Sharif University of Technology
Scientia Iranica
Transactions D: Computer Science & Engineering and Electrical Engineering
http://scientiairanica.sharif.edu

Continuous fixed-time nonsingular terminal sliding mode control of second-order nonlinear systems with matched and mismatched disturbances

A. Khanzadeh and I. Mohammadzaman*

Faculty of Electrical and Computer Engineering, Malek Ashtar University of Technology, Tehran, P.O. Box 15875-1774, Iran.

Received 5 June 2020; received in revised form 13 April 2021; accepted 5 July 2021

KEYWORDS
Fixed-time stability;
Nonsingular terminal sliding mode;
Matched;
Mismatched disturbance.

Abstract. This paper investigates fixed-time nonsingular terminal sliding mode control of second-order nonlinear systems in the presence of matched and mismatched disturbances. Using estimation of the mismatched disturbance estimated by a fixed-time disturbance observer, a novel nonlinear dynamic sliding surface is designed. The convergence time of the closed-loop system including disturbance observer and control system is guaranteed to be uniform with respect to initial conditions. Moreover, the proposed controller avoids chattering phenomenon by producing a continuous control signal.

1. Introduction

Classical Sliding Mode Control (SMC) is a renowned control method owing to its valued attributes such as order reduction, computational simplicity, and inherent robustness against matched disturbances [1]. Nonetheless, it suffers from several drawbacks such as asymptotical stability of the sliding motion and infinitely fast switching, better known as chattering [2]. Furthermore, it is a famous fact about classical SMC that it cannot deal with mismatched disturbances [3,4].

Man and Yu [5] introduced another class of SMC named Terminal Sliding Mode (TSM) and Terminal Sliding Mode Control (TSMC) making use of nonlinear sliding surface to guarantee finite-time convergence of the sliding motion. However, the conventional TSMC causes the singularity problem. This means that in some region of the state space, TSM controller may require to be infinitely large so as to maintain the ideal sliding motion [6]. This problem has been resolved using Nonsingular Terminal Sliding Mode Control (NTSMC) [6–10]. A chatter-free observer-based NTSMC [11] has also been proposed for systems with mismatched disturbances. Though TSMC and NTSMC ensure finite-time stability of the sliding motion, its convergence time depends heavily upon initial conditions that may be unavailable or unknown. The first effort to address this problem of the finite-time stability [12] was made in [13]. Thereafter, the notions of fixed-time stability and control [14–16] are given in the control community literature. Fixed-time stability is finite-time stability whose settling-time function is uniform with respect to the initial conditions.

The first Fixed-Time Nonsingular Terminal Sliding Mode (FTNTSM) and Fixed-Time Nonsingular Terminal Sliding Mode Control (FTNTSMC) was designed by Zou [17]. In this work, the singularity problem is avoided using sinusoidal function. Various FT-NTSM controllers have been proposed in the context of multi-agent systems [18–21]. Corradini and Cristo-

*. *Corresponding author.*
E-mail address: mohammadzaman@mut.ac.ir (I. Mohammadzaman)

doi: 10.24200/sci.2021.56129.4563

faro [22] formulated a class of nonsingular terminal sliding surfaces for designing FTNTSMC of nonlinear planar systems. Disturbance observer-based FTNTSMC of second-order uncertain systems was investigated by Wu et al. [23]. However, all the aforementioned works suffer from chattering. The chattering phenomenon, namely high-frequency oscillations, is the unavoidable result of the classical SMC. Additionally, they considered only matched disturbances while mismatched ones widely appear in practical applications [24–28] and can degrade system performance or even cause instability. Many practical systems such as electromagnetic suspension system, Markovian jump systems, and flexible joint manipulators encounter the issue of mismatched uncertainties and disturbances. In strict terms, controller design dealing with the mismatched uncertainties is technically much more challenging than the case of the matched uncertainties. The attenuation of mismatched disturbances was achieved on the basis of the robust control theory but at a cost of sacrificing the control system performance. As against robust control approach, handling the mismatched disturbances using disturbance-observer-based control technique not only eliminates their effect but also possesses the capability of retrieving the nominal system performance.

Nevertheless, contending with the mismatched disturbances proves to be theoretically much more demanding than matched ones [24], especially when fixed-time control of dynamical systems with mismatched disturbances is encountered. This difficulty substantially increases and unprecedented challenges appear due to the intrinsic complexity of the fixed-time controller design. Therefore, in recent years, only the following papers have been published in this regard. Ni et al. [29] first introduced a uniformly finite-time exact disturbance observer, which brings about reconciliation between the uniform finite-time high-order sliding mode differentiator in [30] and the finite-time disturbance observer in [31]. Then, they proposed a fixed-time observer-based state-feedback controller for stabilization of high-order nonlinear systems with mismatched and matched disturbances. An observer-based FTNTSM controller for reusable launch vehicles despite matched and mismatched disturbances [32] was designed in which the fixed-time nonsingular terminal sliding surface presented in [19] was employed. In this work, while the mismatched disturbance can only be estimated while the matched one is countered by the discontinuous function $sign(\cdot)$, which leads to chattering. The chattering degrades the performance of a control system and can excite unmodeled high-frequency modes of a physical system, which may lead to instability. Therefore, dealing with the matched uncertainties without the chattering is of paramount importance in practise. This can be achieved by benefiting from the disturbance-observer-based control technique. Tian et al. [33] studied the observer-based fixed-time state-feedback stabilizer of high-order integrators using bi-limit homogeneous technique.

Inspired by the above discussion, a complete solution for resolving all the aforementioned problems and making up for all the above-mentioned shortcomings is to reconcile NTSMC with fixed-time stability concept and disturbance observer-based control technique. This solution opens up the possibility that a system is stabilized by an NTSMC within a fixed time and in the presence of the mismatched and matched disturbances without chattering. It should be noted that achieving such a solution leads inevitably to a sophisticated control structure.

This paper investigates observer-based continuous FTNTSMC of second-order nonlinear systems subject to mismatched and matched disturbances. To this end, the uniformly finite-time exact disturbance observer introduced by Ni et al. [29] is employed for estimation of both disturbances. This estimation is utilized in designing a completely novel nonlinear dynamics sliding surface whereby the fixed-time convergence of the sliding motion is guaranteed in spite of mismatched disturbance. Subsequently, a novel observer-based FXNTSMC is introduced in which the singularity problem is avoided using the sinusoidal function. Moreover, the controller is designed in such a way that a continuous control signal is obtained and, in turn, the chattering phenomenon does not occur. As mentioned earlier, this chattering elimination is vital to practical considerations. It is also proven that the phenomenon of escape to infinity in finite time does not arise from the closed-loop system's dynamics in the estimation process during which the observer is trying to converge to the disturbances. Afterwards, the fixed-time stability of the reaching and sliding modes is mathematically shown on the basis of Lyapunov technique. An appealing feature of the proposed controller setting this paper apart the others is that the upper bounds of the convergence time of the reaching and sliding modes explicitly exist as independent design parameters in the control law statement. This offers the possibility that the convergence time of the control system can be set to any desired value in advance. Finally, the proposed controller is applied to the Single Inverted Pendulum (SIP) system in order that the performance of the composite control scheme can be assessed.

2. Preliminaries and problem statement

2.1. Finite-time and fixed-time stability

Consider the following dynamical system:

$$\dot{X} = f(t, X), \qquad X(t_0) = X_0, \tag{1}$$

where $X \in \mathbb{R}^n$, t_0 is the initial time, and $f : \mathbb{R}^+ \times \mathbb{R}^n \to \mathbb{R}^n$ is a continuous, nonlinear function. Assume that the origin is an equilibrium point of Eq. (1). Hereafter, without loss of generality it is assumed that $t_0 = 0$.

Definition 1 [16]. The origin of Eq. (1) is said to be globally finite-time stable if it is globally asymptotically stable and any solution $X(t, X_0)$ of Eq. (1) reaches the equilibria at some finite moment, i.e., $X(t, X_0) = 0$, $\forall\ t \geq T(X_0)$ where $T : \mathbb{R}^n \to \mathbb{R}_+ \cup \{0\}$ is the settling-time function.

Definition 2 [16]. The origin of Eq. (1) is said to be globally fixed-time stable if it is globally finite-time stable and the settling-time function $T(X_0)$ is bounded, i.e., $\exists T_{\max} > 0 : T(X_0) \leq T_{\max}$, $\forall\ X_0 \in \mathbb{R}^n$.

Theorem 1 [16]. If there exists a continuous radially unbounded function $V : \mathbb{R}^n \to \mathbb{R}_+ \cup \{0\}$ such that (i) $V(X) = 0 \Leftrightarrow X = 0$, (ii) any solution of $X(t)$ satisfies the following inequality:

$$\dot{V}(X(t)) \leq -\left(\alpha V^{\eta}(X(t)) + \beta V^{\xi}(X(t))\right)^{k}, \tag{2}$$

where $\alpha, \beta, \eta, \xi, k > 0$ such that $\eta k < 1$ and $\xi k > 1$; then, the origin of Eq. (1) is globally fixed-time stable and the settling-time function satisfies the following inequality:

$$T(X_0) \leq \frac{1}{\alpha^k(1-\eta k)} + \frac{1}{\beta^k(\xi k-1)}, \qquad \forall\ X_0 \in \mathbb{R}^n. \tag{3}$$

As can be seen from Eq. (3), the upper bound of the settling-time function is a nonlinear, complex function of other parameters. This causes the process of tuning the convergence time to be handicapped. However, a special selection of the parameters can make this process effortless as far as possible. Let the parameters be chosen as: $k = \frac{3}{2}$, $\eta = \frac{2}{3}(1 - \frac{q}{p})$, $\xi = \frac{2}{3}(1 - \frac{q}{p}) + \frac{2q}{p}$, and $\alpha = \beta = (\frac{p}{q\mathcal{T}})^{\frac{2}{3}}$. Then, we have:

$$\begin{aligned}\dot{V}(X(t)) &\leq -\left(\alpha V^{\eta}(X(t)) + \beta V^{\xi}(X(t))\right)^{k}\\ &= -\left(\left(\frac{p}{q\mathcal{T}}\right)^{\frac{2}{3}} V^{\frac{2}{3}(1-\frac{q}{p})}(X(t)) + \left(\frac{p}{q\mathcal{T}}\right)^{\frac{2}{3}} \left(V^{\frac{q}{p}}(X(t))\right)^{2} V^{\frac{2}{3}(1-\frac{q}{p})}(X(t))\right)^{\frac{3}{2}}\\ &= -\frac{p}{q\mathcal{T}}\left(1 + \left(V^{\frac{q}{p}}(X(t))\right)^{2}\right)^{\frac{3}{2}} V^{1-\frac{q}{p}}(X(t)),\end{aligned} \tag{4}$$

where p and q are positive, odd integers such that $0 < q/p < 1$ and $\mathcal{T} > 0$. Khanzadeh and Pourgholi [18] proved that the settling-time function of $\dot{V} \leq -\frac{p}{q\mathcal{T}}(1 + (V^{\frac{q}{p}})^2)^{\frac{3}{2}} V^{1-\frac{q}{p}}$ would satisfy $T(X_0) \leq \mathcal{T}$, $\forall\ X_0 \in \mathbb{R}^n$.

2.2. Problem formulation

Consider the following dynamical system under mismatched and matched disturbances described by:

$$\begin{cases}\dot{x}_1 = x_2 + d_1\\ \dot{x}_2 = f(X) + g(X)u + d_2\\ y = x_1\end{cases} \tag{5}$$

where $X = [x_1 x_1]^T \in \mathbb{R}^2$ is the state vector, $u \in \mathbb{R}$ is the control input, $y \in \mathbb{R}$ is the controlled output, and $f(X) \in \mathbb{R}$ and $g(X) \in \mathbb{R}$ are smooth nonlinear functions such that $g(X) \neq 0$ for all $X \in \mathbb{R}^2$. $d_1 \in \mathbb{R}$ and $d_2 \in \mathbb{R}$ denote matched and mismatched disturbances, respectively. It is assumed that the mismatched disturbance d_1 is second-order differentiable and d_1'' has a certain Lipschitz constant.

The goal is to design a continuous FTNTSM controller whereby the output y converges to zero before a prescribed time despite the matched and mismatched disturbances. To this end, a uniformly finite-time exact disturbance observer [29] is initially utilized in order to estimate the disturbances in the system (5) as follows:

$$\begin{aligned}&\dot{z}_{0i} = v_{0i} + h_i, \qquad \dot{z}_{ji} = v_{ji}, \cdots, \dot{z}_{n_i i} = v_{n_i i},\\ &v_{0i} = -k_{0i}\theta|z_{0i} - x_i|^{n_i/(n_i+1)} sign(z_{0i} - x_i)\\ &\qquad - k_{0i}(1-\theta)|z_{0i} - x_i|^{(n_i+1+\alpha)/(n_i+1)}\\ &\qquad sign(z_{0i} - x_i) + z_{1i},\\ &v_{ji} = -k_{ji}\theta|z_{ji} - v_{(j-1)i}|^{(n_i-j)/(n_i-j+1)}\\ &\qquad sign(z_{ji} - v_{(j-1)i})\\ &\qquad - k_{ji}(1-\theta)|z_{0i} - x_i|^{(n_i+1+(j+1)\alpha)/(n_i+1)}\\ &\qquad sign(z_{0i} - x_i) + z_{(j+1)i},\\ &v_{n_i i} = -k_{n_i i}\theta sign(z_{n_i i} - v_{(n_i-1)i})\\ &\qquad - k_{n_i i}(1-\theta)|z_{0i} - x_i|^{(1+\alpha)} sign(z_{0i} - x_i),\end{aligned} \tag{6}$$

where $i = \{1, 2\}$, $h_1 = x_2$, $h_2 = f(X) + g(X)u$, $n_1 = 3$ and $j = 1, \cdots, n_1 - 1$, $n_2 = 2$, α is a sufficiently small positive constant, and $z_{0i}, z_{1i}, \cdots, z_{n_i i}$ are estimation for $x_i, d_i, \cdots, d_i^{(n_i-1)}$, respectively. The observer coefficients k_{ji} are selected according to the condition $|d_i^{(n_i)}| < L_i$ such that the following matrix be Hurwitz.

$$\begin{bmatrix}-k_{0i} & 1 & 0 & \cdots & 0\\ -k_{1i} & 0 & 1 & \cdots & 0\\ \vdots & \vdots & \vdots & \ddots & 0\\ -k_{n_i i} & 0 & 0 & \cdots & 0\end{bmatrix}. \tag{7}$$

The function θ is defined as follows:

$$\theta(t) = \begin{cases} 0 & \text{if } t \leq T_u \\ 1 & \text{if } t > T_u \end{cases} \tag{8}$$

where T_u is a design parameter.

By defining the observer error variables as $e_{0i} = z_{0i} - x_i$, $e_{1i} = z_{1i} - d_i, \cdots, e_{n_i i} = z_{n_i i} - d_i^{(n_i-1)}$, the observer error dynamics is governed by:

$$\begin{cases} \dot{e}_{0i} = -k_{0i}\theta|e_{0i}|^{n_i/(n_i+1)} sign(e_{0i}) \\ \qquad - k_{0i}(1-\theta)|e_{0i}|^{(n_i+1+\alpha)/(n_i+1)} sign(e_{0i}) \\ \qquad + e_{1i} \\ \dot{e}_{1i} = -k_{1i}\theta|e_{1i} - \dot{e}_{0i}|^{(n_i-1)/n_i} sign(e_{1i} - \dot{e}_{0i}) \\ \qquad - k_{1i}(1-\theta)|e_{0i}|^{(n_i+1+2\alpha)/(n_i+1)} sign(e_{0i}) \\ \qquad + e_{2i} \\ \vdots \\ \dot{e}_{(n_i-1)i} = -k_{(n_i-1)i}\theta \left|e_{(n_i-1)i} - \dot{e}_{(n_i-2)i}\right|^{1/2} \\ \qquad sign\left(e_{(n_i-1)i} - \dot{e}_{(n_i-2)i}\right) \\ \qquad - k_{(n_i-1)i}(1-\theta)|e_{0i}|^{(n_i+1+n_i\alpha)/(n_i+1)} \\ \qquad sign(e_{0i}) + e_{n_i i} \\ \dot{e}_{n_i i} = -k_{n_i i}\theta sign\left(e_{n_i i} - \dot{e}_{(n_i-1)i}\right) \\ \qquad - k_{n_i i}(1-\theta)|e_{0i}|^{(1+\alpha)} sign(e_{0i}) \end{cases} \tag{9}$$

Ni el al. [29] proved that the observer error dynamics (9) was fixed-time stable. This implies that e_{ji} for all i's and j's is bounded.

2.3. Mathematical preliminaries

Lemma 1 [11]. If $\xi \in \mathbb{R}$ and $0 < \rho < 1$, it follows:

$$|\xi|^\rho \leq 1 + |\xi|. \tag{10}$$

Lemma 2 [19]. If $x_i \in \mathbb{R}_+ \cup \{0\}$ for $i = 1, \cdots, n$ and $p > 1$, then:

$$n^{1-p}\left(\sum_{i=1}^{n} x_i\right)^p \leq \sum_{i=1}^{n} x_i^p. \tag{11}$$

3. Main results

A novel dynamic nonlinear sliding surface is proposed below:

$$s = \left(x_2 + \hat{d}_1\right)^{\frac{p}{p-2q}} + \left(\frac{p}{2\mathcal{T}_s q}\right)^{\frac{p}{p-2q}} \left(\left(1 + \left((x_1^2)^{\frac{q}{p}}\right)^2\right)^{\frac{3}{2}}\right)^{\frac{p}{p-2q}} x_1, \tag{12}$$

where p and q are positive odd integers such that $p > 8q$, $\mathcal{T}_s > 0$, and $\hat{d}_1 = z_{11}$. The derivative of the sliding surface (12) along the system dynamics (5) is:

$$\dot{s} = \frac{p}{p-2q}\left(\dot{x}_2 + \dot{\hat{d}}_1\right)\left(x_2 + \hat{d}_1\right)^{\frac{2q}{p-2q}} + \left(\frac{p}{2\mathcal{T}_s q}\right)^{\frac{p}{p-2q}} \left(\left(1 + \left((x_1^2)^{\frac{q}{p}}\right)^2\right)^{\frac{3}{2}}\right)^{\frac{p}{p-2q}} (x_2 + d_1) + \frac{6q}{p-2q}\left(\frac{p}{2\mathcal{T}_s q}\right)^{\frac{p}{p-2q}} \left(1 + \left((x_1^2)^{\frac{q}{p}}\right)^2\right)^{\frac{p+4q}{2(p-2q)}} (x_1^2)^{\frac{2q}{p}} (x_2 + d_1), \tag{13}$$

where $\dot{\hat{d}}_1 = z_{21}$. This paper also proposes the following continuous FXNTSMC law:

$$u = -\frac{1}{g(X)}\Bigg(f(X) + \hat{d}_2 + \dot{\hat{d}}_1 + \frac{p-2q}{p}\left(\frac{p}{2\mathcal{T}_s q}\right)^{\frac{p}{p-2q}}\left(x_2 + \hat{d}_1\right)^{(1-\frac{2q}{p-2q})} \times \Bigg[\left(\left(1 + \left((x_1^2)^{\frac{q}{p}}\right)^2\right)^{\frac{3}{2}}\right)^{\frac{p}{p-2q}} + \frac{6q}{p-2q}\left(1 + \left((x_1^2)^{\frac{q}{p}}\right)^2\right)^{\frac{p+4q}{2(p-2q)}} (x_1^2)^{\frac{2q}{p}}\Bigg] + \left(\frac{1}{2}\right)^{1-\frac{\mathcal{Q}}{\mathcal{P}}} \frac{p-2q}{p}\frac{\sqrt{2}\mathcal{P}}{\mathcal{Q}\mathcal{T}_r} \times \mu_\tau\left(\left(x_2 + \hat{d}_1\right)^{\frac{2q}{p-2q}}\right) \left(x_2 + \hat{d}_1\right)^{-(\frac{2q}{p-2q})}\left(1 + \left(\frac{1}{2}s^2\right)^{\frac{3\mathcal{Q}}{\mathcal{P}}}\right) s^{1-\frac{2\mathcal{Q}}{\mathcal{P}}} + \Psi_\tau\left(\left(x_2 + \hat{d}_1\right)^{\frac{2q}{p-2q}}\right)\Bigg), \tag{14}$$

where $\mathcal{P}$ and $\mathcal{Q}$ are positive, odd integers such that $\mathcal{P} > 2(\frac{p}{q} - 2)\mathcal{Q}$, $\mathcal{T}_r > 0$, and $\hat{d}_2 = z_{12}$. The function $\mu_\tau(\cdot)$ [19] is defined for $\tau > 0$ as follows:

$$\mu_\tau(x) = \begin{cases} \sin\left(\frac{\pi}{2}\frac{x^2}{\tau^2}\right), & |x| \leq \tau \\ 1, & \text{otherwise} \end{cases} \tag{15}$$

Since $\mu_\tau(x)/x \to 0$ as $x \to 0$, the control signal (14) is bounded even when $x_2 \to 0$. This guarantees that the control signal is always well-defined. The function $\Psi_\tau(\cdot)$ is also defined as:

$$\Psi_\tau(x) = \begin{cases} \psi sign(s), & |x| \leq \tau, \quad s \neq 0 \\ 0, & \text{otherwise} \end{cases} \tag{16}$$

where $\psi > 0$.

Theorem 2. Consider the second-order dynamical system (5). If the control law is established as Eq. (14), then the system output $y = x_1$ will converge to zero within a fixed time and settling-time function $T(X_0)$ satisfies:

$$T(X_0) \le \mathcal{T}_{obs} + \mathcal{T}_s + \mathcal{T}_r, \tag{17}$$

where $\mathcal{T}_{obs}$ is assumed to be the upper bound of convergence time of observer, $\mathcal{T}_r$ is that of the reaching mode, and $\mathcal{T}_s$ is that of the sliding mode.

Proof. First, it is necessary to prove that during the process of disturbances estimated by the system of Eqs. (6), the closed-loop system will not escape in a finite time horizon.

Substituting the control law (14) into Eq. (13) yields:

$$\dot{s} = \frac{-p}{p-2q} e_2 \tilde{x}_2^{\frac{2q}{p-2q}} - \left(\frac{p}{2\mathcal{T}_s q}\right)^{\frac{p}{p-2q}} \left(\left(1+\left((x_1^2)^{\frac{q}{p}}\right)^2\right)^{\frac{3}{2}}\right)^{\frac{p}{p-2q}} e_1 - \frac{6q}{p-2q} \left(\frac{p}{2\mathcal{T}_s q}\right)^{\frac{p}{p-2q}} \left(1+\left((x_1^2)^{\frac{q}{p}}\right)^2\right)^{\frac{p+4q}{2(p-2q)}} (x_1^2)^{\frac{2q}{p}} e_1 - \left(\frac{1}{2}\right)^{1-\frac{\mathcal{Q}}{\mathcal{P}}} \frac{\sqrt{2}\mathcal{P}}{\mathcal{Q}\mathcal{T}_r} \mu_\tau \left(\tilde{x}_2^{\frac{2q}{p-2q}}\right) \left(1+\left(\frac{1}{2}s^2\right)^{\frac{3\mathcal{Q}}{\mathcal{P}}}\right) s^{1-\frac{2\mathcal{Q}}{\mathcal{P}}} - \frac{p}{p-2q}\left(x_2+\hat{d}_1\right)^{\frac{2q}{p-2q}} \Psi_\tau\left((x_2+\hat{d}_1)^{\frac{2q}{p-2q}}\right), \tag{18}$$

where $e_1 = \hat{d}_1 - d_1$, $e_2 = \hat{d}_2 - d_2$, and $\tilde{x}_2 = x_2 + d_1$. Multiplying both sides of Eq. (18) by s results in:

$$s\dot{s} = \frac{-p}{p-2q} s e_2 \tilde{x}_2^{\frac{2q}{p-2q}} - \left(\frac{p}{2\mathcal{T}_s q}\right)^{\frac{p}{p-2q}} \left(\left(1+\left((x_1^2)^{\frac{q}{p}}\right)^2\right)^{\frac{3}{2}}\right)^{\frac{p}{p-2q}} s e_1 - \frac{6q}{p-2q} \left(\frac{p}{2\mathcal{T}_s q}\right)^{\frac{p}{p-2q}} \left(1+\left((x_1^2)^{\frac{q}{p}}\right)^2\right)^{\frac{p+4q}{2(p-2q)}} (x_1^2)^{\frac{2q}{p}} s e_1 - \left(\frac{1}{2}\right)^{1-\frac{\mathcal{Q}}{\mathcal{P}}} \frac{\sqrt{2}\mathcal{P}}{\mathcal{Q}\mathcal{T}_r} \mu_\tau \left(\tilde{x}_2^{\frac{2q}{p-2q}}\right) \left(1+\left(\frac{1}{2}s^2\right)^{\frac{3\mathcal{Q}}{\mathcal{P}}}\right) (s^2)^{1-\frac{\mathcal{Q}}{\mathcal{P}}} - \frac{p}{p-2q} s\tilde{x}_2^{\frac{2q}{p-2q}} \Psi_\tau\left(\tilde{x}_2^{\frac{2q}{p-2q}}\right) \le \frac{p}{p-2q}|s||e_2|\tilde{x}_2^{\frac{2q}{p-2q}} + \left(\frac{p}{2\mathcal{T}_s q}\right)^{\frac{p}{p-2q}} \left(\left(1+\left((x_1^2)^{\frac{q}{p}}\right)^2\right)^{\frac{3}{2}}\right)^{\frac{p}{p-2q}} |s||e_1| + \frac{6q}{p-2q}\left(\frac{p}{2\mathcal{T}_s q}\right)^{\frac{p}{p-2q}} \left(1+\left((x_1^2)^{\frac{q}{p}}\right)^2\right)^{\frac{p+4q}{2(p-2q)}} (x_1^2)^{\frac{2q}{p}} |s||e_1|. \tag{19}$$

From Lemma 1 and since $p > 8q$, it follows $\tilde{x}_2^{\frac{2q}{p-2q}} < 1 + |\tilde{x}_2|$:

$$\left(\left(1+\left((x_1^2)^{\frac{q}{p}}\right)^2\right)^{\frac{3}{2}}\right)^{\frac{p}{p-2q}} < \left(1+x_1^{\frac{4q}{p}}\right)^{\frac{3p}{2(p-2q)}} < \left(1+x_1^{\frac{4q}{p}}\right)^2 = 1+2x_1^{\frac{4q}{p}}+x_1^{\frac{8q}{p}} < 4+3|x_1|, \tag{20}$$

and:

$$\left(1+\left((x_1^2)^{\frac{q}{p}}\right)^2\right)^{\frac{p+4q}{2(p-2q)}} (x_1^2)^{\frac{2q}{p}} < \left(2+x_1^{\frac{4q}{p}}\right) x_1^{\frac{4q}{p}} = 2x_1^{\frac{4q}{p}} + x_1^{\frac{8q}{p}} < 3(1+|x_1|). \tag{21}$$

Thus, we have:

$$s\dot{s} \le \frac{p}{p-2q}|s||e_2|\left(1+|\tilde{x}_2|\right) + \left(\frac{p}{2\mathcal{T}_s q}\right)^{\frac{p}{p-2q}} (4+3|x_1|)|s||e_1| + \frac{18q}{p-2q}\left(\frac{p}{2\mathcal{T}_s q}\right)^{\frac{p}{p-2q}} (1+|x_1|)|s||e_1|. \tag{22}$$

Given that $|a||b| \le \frac{a^2+b^2}{2}$ yields:

$$s\dot{s} \le \frac{p}{p-2q}\left(\frac{e_2^2+s^2}{2} + |e_2|\frac{\tilde{x}_2^2+s^2}{2}\right) + \left(\frac{p}{2\mathcal{T}_s q}\right)^{\frac{p}{p-2q}} \left(4\frac{e_1^2+s^2}{2} + 3|e_1|\frac{x_1^2+s^2}{2}\right) + \frac{18q}{p-2q}\left(\frac{p}{2\mathcal{T}_s q}\right)^{\frac{p}{p-2q}} \left(\frac{e_1^2+s^2}{2} + |e_1|\frac{x_1^2+s^2}{2}\right) = \Gamma_1 + \Gamma_2\frac{x_1^2}{2} + \Gamma_3\frac{\tilde{x}_2^2}{2} + \Gamma_4\frac{s^2}{2}, \tag{23}$$

where:

$$\Gamma_1 = \frac{1}{2}\left(\frac{p}{p-2q}e_2^2 + \left(\frac{p}{2\mathcal{T}_s q}\right)^{\frac{p}{p-2q}} \left(4+\frac{18q}{p-2q}\right) e_1^2\right),$$

$$\Gamma_2 = \left(\frac{p}{2\mathcal{T}_s q}\right)^{\frac{p}{p-2q}} |e_1| \left(3+\frac{18q}{p-2q}\right),$$

$$\Gamma_3 = \frac{p}{p-2q}|e_2|,$$

and:

$$\Gamma_4 = \frac{p}{p-2q}(1+|e_2|) + \left(\frac{p}{2\mathcal{T}_s q}\right)^{\frac{p}{p-2q}} \left((4+3|e_1|) + \frac{18q}{p-2q}(1+|e_1|)\right).$$

The dynamics of $\tilde{x}_2$ is given by:

$$\dot{\tilde{x}}_2 = f(X) + g(X)u + d_2\dot{\hat{d}}_1. \tag{24}$$

Substituting the control law (14) into Eq. (24) yields:

$$\dot{\tilde{x}}_2 = -e_2 - \frac{p-2q}{p}\left(\frac{p}{2\mathcal{T}_s q}\right)^{\frac{p}{p-2q}} \left(\left(1+\left((x_1^2)^{\frac{q}{p}}\right)^2\right)^{\frac{3}{2}}\right)^{\frac{p}{p-2q}} \tilde{x}_2^{\left(1-\frac{2q}{p-2q}\right)} - \frac{6q}{p}\left(\frac{p}{2\mathcal{T}_s q}\right)^{\frac{p}{p-2q}} \left(1+\left((x_1^2)^{\frac{q}{p}}\right)^2\right)^{\frac{p+4q}{2(p-2q)}} (x_1^2)^{\frac{2q}{p}} \tilde{x}_2^{\left(1-\frac{2q}{p-2q}\right)} - \left(\frac{1}{2}\right)^{1-\frac{\mathcal{Q}}{\mathcal{P}}} \frac{p-2q}{p}\frac{\sqrt{2}\mathcal{P}}{\mathcal{Q}\mathcal{T}_r} \mu_\tau\left(\tilde{x}_2^{\frac{2q}{p-2q}}\right) \tilde{x}_2^{-\left(\frac{2q}{p-2q}\right)} \left(1+\left(\frac{1}{2}s^2\right)^{\frac{3\mathcal{Q}}{\mathcal{P}}}\right) s^{1-\frac{2\mathcal{Q}}{\mathcal{P}}} - \Psi_\tau\left(\tilde{x}_2^{\frac{2q}{p-2q}}\right). \tag{25}$$

Multiplying both sides of Eq. (25) by $\tilde{x}_2$ results in:

$$\tilde{x}_2\dot{\tilde{x}}_2 = -e_2\tilde{x}_2 - \frac{p-2q}{p}\left(\frac{p}{2\mathcal{T}_s q}\right)^{\frac{p}{p-2q}} \left(\left(1+\left((x_1^2)^{\frac{q}{p}}\right)^2\right)^{\frac{3}{2}}\right)^{\frac{p}{p-2q}} (\tilde{x}_2^2)^{\left(1-\frac{q}{p-2q}\right)} - \frac{6q}{p}\left(\frac{p}{2\mathcal{T}_s q}\right)^{\frac{p}{p-2q}} \left(1+\left((x_1^2)^{\frac{q}{p}}\right)^2\right)^{\frac{p+4q}{2(p-2q)}} (x_1^2)^{\frac{2q}{p}} (\tilde{x}_2^2)^{\left(1-\frac{q}{p-2q}\right)} - \left(\frac{1}{2}\right)^{1-\frac{\mathcal{Q}}{\mathcal{P}}} \frac{p-2q}{p}\frac{\sqrt{2}\mathcal{P}}{\mathcal{Q}\mathcal{T}_r}\mu_\tau\left(\tilde{x}_2^{\frac{2q}{p-2q}}\right)\tilde{x}_2^{1-\left(\frac{2q}{p-2q}\right)} \left(s^{1-\frac{2\mathcal{Q}}{\mathcal{P}}} + \left(\frac{1}{2}s^2\right)^{\frac{3\mathcal{Q}}{\mathcal{P}}} s^{1-\frac{2\mathcal{Q}}{\mathcal{P}}}\right) - \tilde{x}_2\Psi_\tau\left(\tilde{x}_2^{\frac{2q}{p-2q}}\right) \leq |e_2||\tilde{x}_2| + \left(\frac{1}{2}\right)^{1-\frac{\mathcal{Q}}{\mathcal{P}}} \frac{p-2q}{p}\frac{\sqrt{2}\mathcal{P}}{\mathcal{Q}\mathcal{T}_r}\left(|\tilde{x}_2|^{1-\left(\frac{2q}{p-2q}\right)}|s|^{1-\frac{2\mathcal{Q}}{\mathcal{P}}} + \left(\frac{1}{2}\right)^{\frac{3\mathcal{Q}}{\mathcal{P}}}|\tilde{x}_2|^{1-\left(\frac{2q}{p-2q}\right)}|s|^{1+\frac{4\mathcal{Q}}{\mathcal{P}}}\right) + |\tilde{x}_2|\left|\Psi_\tau\left(\tilde{x}_2^{\frac{2q}{p-2q}}\right)\right|. \tag{26}$$

It follows from Lemma 1 that $|\tilde{x}_2|^{1-\left(\frac{2q}{p-2q}\right)} < 1+|\tilde{x}_2|$ and $|s|^{1-\frac{2\mathcal{Q}}{\mathcal{P}}} < 1+|s|$. According to Eq. (16), it can be concluded that $|\tilde{x}_2||\Psi_\tau(\tilde{x}_2^{\frac{2q}{p-2q}})| \leq \psi|\tilde{x}_2| < \psi(1+\tilde{x}_2^2)$. In the case of $\max\{|\tilde{x}_2|,|s|\} \leq 1$, it is obvious that $|\tilde{x}_2|^{1-\left(\frac{2q}{p-2q}\right)}|s|^{1+\frac{4\mathcal{Q}}{\mathcal{P}}} \leq 1$. In the case of $\min\{|\tilde{x}_2|,|s|\} > 1$, it follows $|\tilde{x}_2|^{1-\left(\frac{2q}{p-2q}\right)}|s|^{1+\frac{4\mathcal{Q}}{\mathcal{P}}} \leq (\tilde{x}_2^2)^{1-\left(\frac{q}{p-2q}-\frac{2\mathcal{Q}}{\mathcal{P}}\right)} < \tilde{x}_2^2$ if $|\tilde{x}_2| \geq |s|$ and $|\tilde{x}_2|^{1-\left(\frac{2q}{p-2q}\right)}|s|^{1+\frac{4\mathcal{Q}}{\mathcal{P}}} \leq (s^2)^{1-\left(\frac{q}{p-2q}-\frac{2\mathcal{Q}}{\mathcal{P}}\right)} < s^2$ if $|s| \geq |\tilde{x}_2|$. Combining both cases together and using $|a||b| \leq \frac{a^2+b^2}{2}$ yield the following:

$$\tilde{x}_2\dot{\tilde{x}}_2 \leq |e_2||\tilde{x}_2| + \left(\frac{1}{2}\right)^{1-\frac{\mathcal{Q}}{\mathcal{P}}} \frac{p-2q}{p}\frac{\sqrt{2}\mathcal{P}}{\mathcal{Q}\mathcal{T}_r}\left(1+|\tilde{x}_2| + |s| + |\tilde{x}_2||s| + \left(\frac{1}{2}\right)^{\frac{3\mathcal{Q}}{\mathcal{P}}}\left(1+\frac{\tilde{x}_2^2}{2}+\frac{s^2}{2}\right)\right) + \psi\left(1+\tilde{x}_2^2\right) \leq \frac{e_2^2+\tilde{x}_2^2}{2} + \left(\frac{1}{2}\right)^{1-\frac{\mathcal{Q}}{\mathcal{P}}}\frac{p-2q}{p}\frac{\sqrt{2}\mathcal{P}}{\mathcal{Q}\mathcal{T}_r}\left(1+\frac{1+\tilde{x}_2^2}{2}+\frac{1+s^2}{2}+\frac{\tilde{x}_2^2+s^2}{2} + \left(\frac{1}{2}\right)^{\frac{3\mathcal{Q}}{\mathcal{P}}}\left(1+\frac{\tilde{x}_2^2}{2}+\frac{s^2}{2}\right)\right) + \psi\left(1+\tilde{x}_2^2\right) = \Gamma_5 + \Gamma_6\frac{\tilde{x}_2^2}{2} + \Gamma_7\frac{s^2}{2}, \tag{27}$$

where:

$$\Gamma_5 = \frac{e_2^2}{2} + \psi + \left(\frac{1}{2}\right)^{1-\frac{\mathcal{Q}}{\mathcal{P}}}\frac{p-2q}{p}\frac{\sqrt{2}\mathcal{P}}{\mathcal{Q}\mathcal{T}_r}\left(2+\left(\frac{1}{2}\right)^{\frac{3\mathcal{Q}}{\mathcal{P}}}\right),$$

$$\Gamma_6 = 1+2\psi + \left(\frac{1}{2}\right)^{1-\frac{\mathcal{Q}}{\mathcal{P}}}\frac{p-2q}{p}\frac{\sqrt{2}\mathcal{P}}{\mathcal{Q}\mathcal{T}_r}\left(2+\left(\frac{1}{2}\right)^{\frac{3\mathcal{Q}}{\mathcal{P}}}\right),$$

and:

$$\Gamma_7 = \left(\frac{1}{2}\right)^{1-\frac{\mathcal{Q}}{\mathcal{P}}}\frac{p-2q}{p}\frac{\sqrt{2}\mathcal{P}}{\mathcal{Q}\mathcal{T}_r}\left(2+\left(\frac{1}{2}\right)^{\frac{3\mathcal{Q}}{\mathcal{P}}}\right).$$

The dynamics of x_1 can also be written as $\dot{x}_1 = x_2 + d_1 = x_2 + \hat{d}_1 + d_1 - \hat{d}_1 = \tilde{x}_2 - e_1$. Accordingly, it follows:

$$x_1\dot{x}_1 = x_1\tilde{x}_2 - x_1 e_1 \le |x_1|\,|\tilde{x}_2| + |x_1||e_1|$$

$$\le \frac{x_1^2+\tilde{x}_2^2}{2} + \frac{x_1^2+e_1^2}{2} = \Gamma_8 + \Gamma_9\frac{x_1^2}{2} + \Gamma_{10}\frac{\tilde{x}_2^2}{2}, \quad (28)$$

where $\Gamma_8 = \frac{e_1^2}{2}$, $\Gamma_9 = 2$, and $\Gamma_{10} = 1$.

Based on the work of Li and Tian [34], let us define a finite time bounded function $V_{cl}(x_1, \tilde{x}_2, s) = \frac{1}{2}(x_1^2 + \tilde{x}_2^2 + s^2)$ for the sliding surface dynamics (18) and the state dynamics (5). In accordance with Inequalities (23), (27), and (28), the derivative of V_{cl} along the state dynamics (5) satisfies:

$$\dot{V}_{cl} = x_1\dot{x}_1 + \tilde{x}_2\dot{\tilde{x}}_2 + s\dot{s} \le (\Gamma_1+\Gamma_5+\Gamma_8) + (\Gamma_2+\Gamma_9)\frac{x_1^2}{2} + (\Gamma_3+\Gamma_6+\Gamma_{10})\frac{\tilde{x}_2^2}{2} + (\Gamma_4+\Gamma_7)\frac{s^2}{2}. \quad (29)$$

The coefficients Γ_i for $i = 1, \cdots, 10$ are bounded due to the boundness of e_1 and e_2. By defining $\Gamma_{Cons} = \Gamma_1 + \Gamma_5 + \Gamma_8$, $\Gamma_{\max} = \max\{\Gamma_2+\Gamma_9, \Gamma_3+\Gamma_6+\Gamma_{10}, \Gamma_4+\Gamma_7\}$, the following result is obtained:

$$\dot{V}_{cl} \le \Gamma_{Cons} + \Gamma_{\max}V_{cl}. \quad (30)$$

It can be concluded from Inequality (30) that V_{cl} and x_1, $\tilde{x}_2$, and s will not escape to infinity in finite time [34].

Since the estimation of disturbances e_1 and e_2 in Eq. (9) converges to zero within a finite time upper bound by a constant $\mathcal{T}_{obs}$, the sliding surface dynamics (18), for $t \ge \mathcal{T}_{obs}$, will reduce to:

$$\dot{s} = -\left(\frac{1}{2}\right)^{1-\frac{\mathcal{Q}}{\mathcal{P}}} \frac{\sqrt{2}\mathcal{P}}{\mathcal{Q}\mathcal{T}_r}\mu_\tau\left(\tilde{x}_2^{\frac{2q}{p-2q}}\right)\left(1+\left(\frac{1}{2}s^2\right)^{\frac{3\mathcal{Q}}{\mathcal{P}}}\right) s^{1-\frac{2\mathcal{Q}}{\mathcal{P}}} - \frac{p}{p-2q}\tilde{x}_2^{\frac{2q}{p-2q}}\Psi_\tau\left(\tilde{x}_2^{\frac{2q}{p-2q}}\right). \quad (31)$$

Define $V_r = \frac{1}{2}s^2$. Taking derivative of V_r and using Eq. (31) yield the following:

$$\dot{V}_r = s\dot{s} = -\frac{\sqrt{2}\mathcal{P}}{\mathcal{Q}\mathcal{T}_r}\mu_\tau\left(\tilde{x}_2^{\frac{2q}{p-2q}}\right)\left(1+(V_r)^{\frac{3\mathcal{Q}}{\mathcal{P}}}\right)(V_r)^{1-\frac{\mathcal{Q}}{\mathcal{P}}} - \frac{p}{p-2q}s\tilde{x}_2^{\frac{2q}{p-2q}}\Psi_\tau\left(\tilde{x}_2^{\frac{2q}{p-2q}}\right). \quad (32)$$

As is clear from the definition of Ψ_τ, then:

$$-\frac{p}{p-2q}s\tilde{x}_2^{\frac{2q}{p-2q}}\Psi_\tau(\tilde{x}_2^{\frac{2q}{p-2q}}) = -\frac{p}{p-2q}\psi|s|\tilde{x}_2^{\frac{2q}{p-2q}},$$

when:

$$s \ne 0, \quad \tilde{x}_2^{\frac{2q}{p-2q}} \le \tau,$$

$$-\frac{p}{p-2q}s\tilde{x}_2^{\frac{2q}{p-2q}}\Psi_\tau(\tilde{x}_2^{\frac{2q}{p-2q}}) = 0.$$

Accordingly, $-\frac{p}{p-2q}s\tilde{x}_2^{\frac{2q}{p-2q}}\Psi_\tau(\tilde{x}_2^{\frac{2q}{p-2q}}) \le 0$ holds true $\forall\ \tilde{x}_2, s \in \mathbb{R}$. Hence, the following result is obtained based on Lemma 2:

$$\begin{aligned}
\dot{V}_r &\le -\frac{\sqrt{2}\mathcal{P}}{\mathcal{Q}\mathcal{T}_r}\mu_\tau\left(\tilde{x}_2^{\frac{2q}{p-2q}}\right)\left(1+(V_r)^{\frac{3\mathcal{Q}}{\mathcal{P}}}\right)(V_r)^{1-\frac{\mathcal{Q}}{\mathcal{P}}} \\
&= -\frac{\sqrt{2}\mathcal{P}}{\mathcal{Q}\mathcal{T}_r}\mu_\tau\left(\tilde{x}_2^{\frac{2q}{p-2q}}\right)\left(\left(\left(V_r^{\frac{2}{3}(1-\frac{\mathcal{Q}}{\mathcal{P}})}\right)\right)^{\frac{3}{2}} + \left(\left(V_r^{\frac{\mathcal{Q}}{\mathcal{P}}}\right)^2 V_r^{\frac{2}{3}(1-\frac{\mathcal{Q}}{\mathcal{P}})}\right)^{\frac{3}{2}}\right) \\
&\le -\frac{\mathcal{P}}{\mathcal{Q}\mathcal{T}_r}\mu_\tau\left(\tilde{x}_2^{\frac{2q}{p-2q}}\right)\left(V_r^{\frac{2}{3}(1-\frac{\mathcal{Q}}{\mathcal{P}})} + \left(V_r^{\frac{\mathcal{Q}}{\mathcal{P}}}\right)^2 V_r^{\frac{2}{3}(1-\frac{\mathcal{Q}}{\mathcal{P}})}\right)^{\frac{3}{2}} \\
&= -\frac{\mathcal{P}}{\mathcal{Q}\mathcal{T}_r}\mu_\tau\left(\tilde{x}_2^{\frac{2q}{p-2q}}\right)\left(1+\left(V_r^{\frac{\mathcal{Q}}{\mathcal{P}}}\right)^2\right)^{\frac{3}{2}} V_r^{1-\frac{\mathcal{Q}}{\mathcal{P}}}.
\end{aligned} \quad (33)$$

Let us divide the phase plane whose axes are defined by x_1 and $\tilde{x}_2$ into three regions $\mathcal{R}_1 = \{(x_1, \tilde{x}_2)^T \in \mathbb{R}^2 | |\tilde{x}_2^{\frac{2q}{p-2q}}| > \tau, s \ne 0\}$, $\mathcal{R}_2 = \{(x_1, \tilde{x}_2)^T \in \mathbb{R}^2 | |\tilde{x}_2^{\frac{2q}{p-2q}}| \le \tau, s \ne 0\}$, and $\mathcal{R}_3 = \{(x_1, \tilde{x}_2)^T \in \mathbb{R}^2 | s = 0\}$ (Figure 1). In $\mathcal{R}_1$, it follows from $\mu_\tau(\tilde{x}_2^{\frac{2q}{p-2q}}) = 1$ that $\dot{V}_r \le -\frac{\mathcal{P}}{\mathcal{Q}\mathcal{T}_r}(1+(V_r^{\frac{\mathcal{Q}}{\mathcal{P}}})^2)^{\frac{3}{2}}V_r^{1-\frac{\mathcal{Q}}{\mathcal{P}}}$. As a consequence, the state trajectory will either directly reach the sliding surface s or enter $\mathcal{R}_2$. Assume τ to be chosen sufficiently small. In $\mathcal{R}_2$, it results from Eq. (25) that the dynamics of $\tilde{x}_2$ is governed by $\dot{\tilde{x}}_2 = -\Psi_\tau\left(\tilde{x}_2^{\frac{2q}{p-2q}}\right) = -\psi sign(s)$ because $\mu_\tau(\tilde{x}_2^{\frac{2q}{p-2q}})\tilde{x}_2^{-(\frac{2q}{p-2q})} \to 0$ as $\tilde{x}_2 \to 0$. This means $\dot{\tilde{x}}_2 = \psi$ for $s < 0$ and $\dot{\tilde{x}}_2 = -\psi$ for $s >$

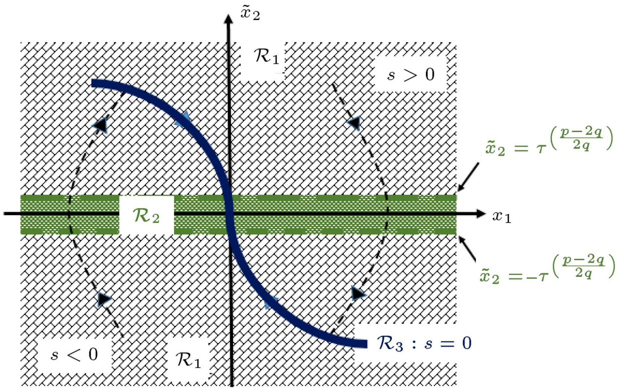

Figure 1. Phase plane plot.

0. This dynamic guarantees that the state trajectory crosses $\mathcal{R}_2$ within finite time $\frac{2\tau^{(p-2q)/2q}}{\psi}$ and, then, is directed to the sliding surface by $\dot{V}_r \leq -\frac{\mathcal{P}}{\mathcal{Q}\mathcal{T}_r}(1+(V_r^{\frac{\mathcal{Q}}{\mathcal{P}}})^2)^{\frac{3}{2}} V_r^{1-\frac{\mathcal{Q}}{\mathcal{P}}}$. Therefore, the state trajectory will ultimately reach the sliding surface at most within the period $\mathcal{T}_r + \frac{2\tau^{(p-2q)/2q}}{\psi}$. If ψ is chosen sufficiently large, the term $\frac{2\tau^{(p-2q)/2q}}{\psi}$ can entirely be neglected. Accordingly, for $t \geq \mathcal{T}_{obs} + \mathcal{T}_r$, the sliding motion begins. In $\mathcal{R}_3$, it follows:

$$0 = \left(x_2 + \hat{d}_1\right)^{\frac{p}{p-2q}} + \left(\frac{p}{2\mathcal{T}_s q}\right)^{\frac{p}{p-2q}} \left(\left(1+\left((x_1^2)^{\frac{q}{p}}\right)^2\right)^{\frac{3}{2}}\right)^{\frac{p}{p-2q}} x_1. \tag{34}$$

Since $\hat{d}_1 = d_1$ for $t \geq \mathcal{T}_{obs}$, $x_2 + \hat{d}_1 = x_2 + d_1 = \dot{x}_1$. Thus, the sliding motion dynamic is governed by:

$$\dot{x}_1 = -\frac{p}{2\mathcal{T}_s q}\left(1+\left((x_1^2)^{\frac{q}{p}}\right)^2\right)^{\frac{3}{2}} x_1^{1-\frac{2q}{p}}. \tag{35}$$

Here, we define $V_s = x_1^2$. Taking derivative of V_s and using Eq. (35) yield the following:

$$\dot{V}_s = 2x_1\dot{x}_1 = -\frac{p}{\mathcal{T}_s q}\left(1+\left(V_s^{\frac{q}{p}}\right)^2\right)^{\frac{3}{2}} V_s^{1-\frac{q}{p}}. \tag{36}$$

This guarantees that in the sliding motion, x_1 converges to the origin at most within the period $\mathcal{T}_s$. As per what was gathered, the system output y converged to the origin from any initial state in the state space and the settling-time function satisfies $T(X_0) \leq \mathcal{T}_{obs} + \mathcal{T}_s + \mathcal{T}_r$, which completes the proof. ■

Remark 1. Once the state trajectory comes into the region $\mathcal{R}_2$, the function $\Psi_\tau(\cdot)$ in the control law statement (14) drives it to cross $\mathcal{R}_2$ within finite time. In strict terms, this function ensures that $\tilde{x}_2 = 0$ will not be attractor. It should also be noticed that the condition $s \neq 0$ of $\Psi_\tau(\cdot)$ is necessary for the continuity of the control signal because it does not allow chattering to occur in $\mathcal{R}_c = \mathcal{R}_2 \cap \mathcal{R}_3$, which is depicted in Figure 2.

Remark 2. As was proven earlier, $\mathcal{T}_r$ and $\mathcal{T}_s$ are upper bounds of convergence time of the reaching and sliding modes, respectively. They explicitly exist as independent design parameters in the control law statement (14). This enables us to set them to any desired value in advance. These design parameters determine the convergence speed of the output. The smaller these parameters are chosen, the faster the output converges to the zero. The parameter τ determines the thickness

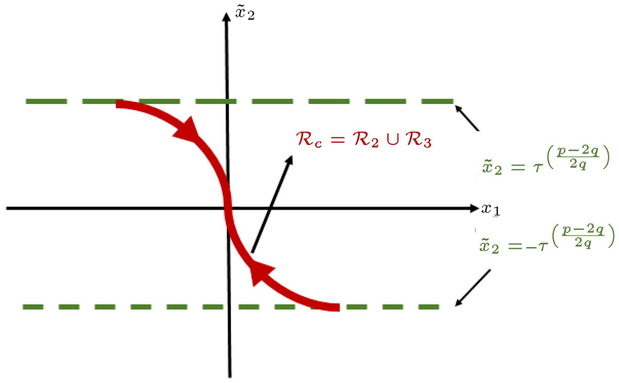

Figure 2. The region $\mathcal{R}_c = \mathcal{R}_2 \cap \mathcal{R}_3$.

of the region $\mathcal{R}_2$. This parameter must be chosen sufficiently small in order that the negligibility of the term $\frac{2\tau^{(p-2q)/2q}}{\psi}$ can be guaranteed. Choosing large values for the parameter ψ is also necessary for making the term $\frac{2\tau^{(p-2q)/2q}}{\psi}$ smaller.

4. Simulation results

This section is to represent a numerical simulation. A benchmark simulation example is SIP system [17] whose intrinsic instability and fast dynamics can show how effective a control system acts. Hence, the proposed controller (14) is applied to the SIP system when the controller's parameters are selected as $q = 1$, $p = 9$, $\mathcal{Q} = 1$, $\mathcal{P} = 15$, $\tau = 0.1$, $\mathcal{T}_r = \mathcal{T}_s = 5$, $\psi = 5$ and the initial conditions are set as $x_1(0) = 0.5$, $x_2(0) = 0.5$. The disturbances are considered as $d_1 = 0.5\sin 2t + 0.5\cos x_1(t)$, $d_2 = 0.5\cos 3t + 0.5\sin x_2(t)$ and the observer's parameters are chosen as $z_{01} = z_{11} = z_{21} = z_{31} = z_{02} = z_{12} = z_{22} = 1$, $k_{01} = 5$, $k_{11} = k_{21} = 10$, $k_{31} = 4$, $k_{02} = 5$, $k_{12} = 10$, $k_{22} = 7$, $T_u = 0.1$, $\alpha = 0.01$. Figures 3 and 4 show that the observer's state variables converge to the disturbances d_1 and d_2 approximately at $t = 2$ s. The response curve of the output $y = x_1$ is depicted in Figure 5. This figure indicates that the overall closed-loop system has been successful in stabilizing the output since x_1 has converged to zero before the time $\mathcal{T}_r + \mathcal{T}_s = 10$.

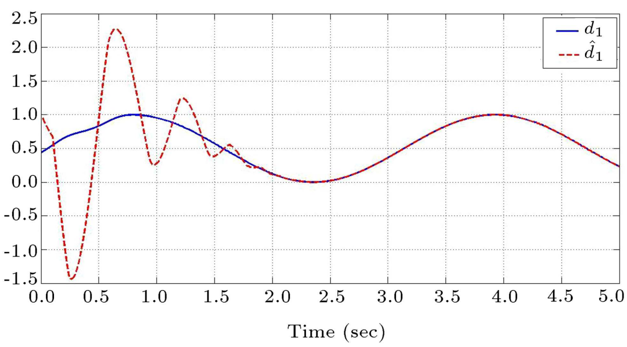

Figure 3. Response curve of d_1 and $\hat{d}_1$.

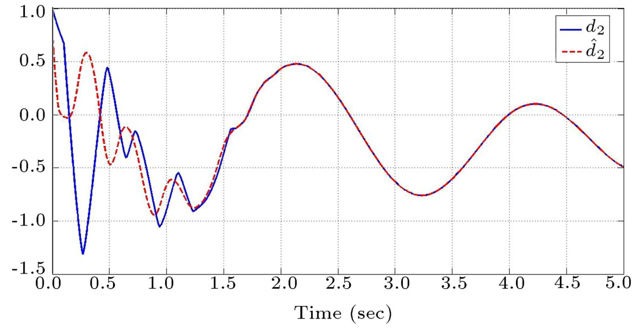

Figure 4. Response curve of d_2 and $\hat{d}_2$.

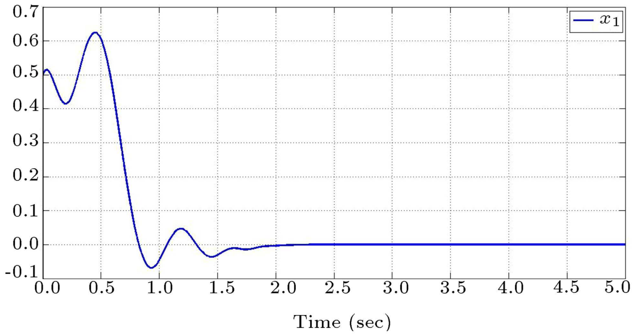

Figure 5. Response curve of $y = x_1$.

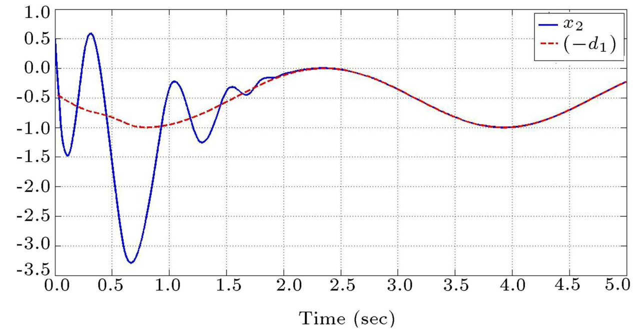

Figure 6. Response curve of x_2 and $(-d_1)$.

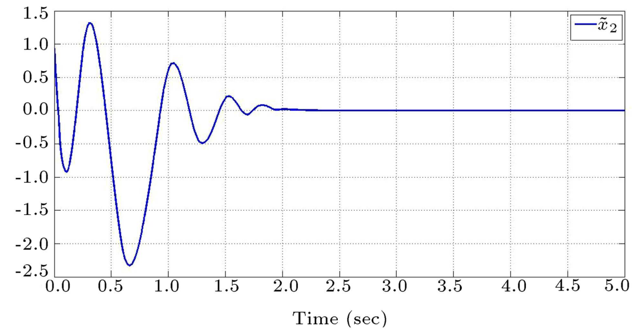

Figure 7. Response curve of $\tilde{x}_2$.

Figure 6 shows that the state variable x_2 has converged to $(-d_1)$, which is equivalent to the convergence of $\tilde{x}_2$ to zero (Figure 7). The behavior of the sliding surface is depicted in Figure 8. As can clearly be understood from this figure, the sliding surface is driven into zero before the time $\mathcal{T}_r = 5$. The control signal u is shown

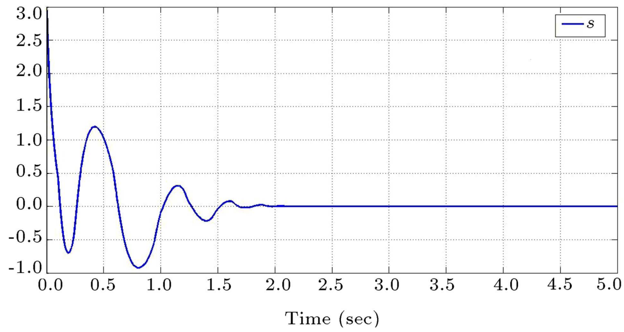

Figure 8. Response curve of the switching surface s.

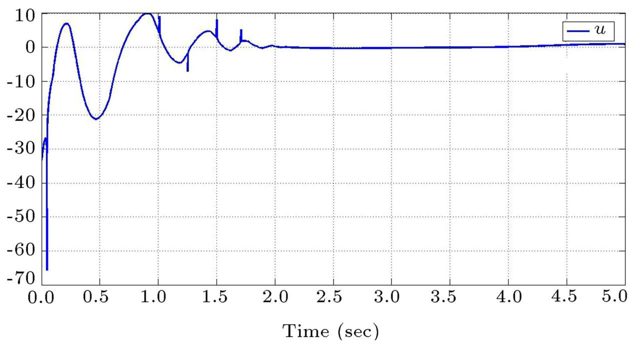

Figure 9. Response curve of the control signal.

in Figure 9. This figure bears witness to the fact that the control signal is continuous.

To demonstrate the effectiveness of the proposed method, the controller is compared with the fixed-time sliding mode controller introduced by Jianguo and Shengjiang [35]. We have chosen the aforementioned paper because its idea is somewhat similar to what was proposed here; however, these two papers essentially adopted different approaches to constructing a fixed-time sliding mode controller. In strict terms, Jianguo and Shengjiang's controller was designed on the basis of ordinary fixed-time control method, while the proposed controller was derived from a completely novel and different approach.

Unlike the claim of the authors of the above-mentioned paper, their proposed fixed-time sliding mode controller is not fixed-time stable. This can easily be evidenced by the formula [35, page 3]:

$$T_1 = \frac{\ln\left(\frac{s(0)k_1}{\left(k_{21} - \frac{\delta d^*}{\eta}\right)} + 1\right)}{k_1},$$

obtained for the convergence time of the reaching phase. This formula clearly shows that the convergence time of the reaching phase depends on the initial conditions $s(0)$, which is completely contrary to the concepts of the fixed-time stability and control. In addition, the aforementioned paper has only considered the mismatched uncertainties and used a linear observer rather than a fixed-time one. Nonetheless,

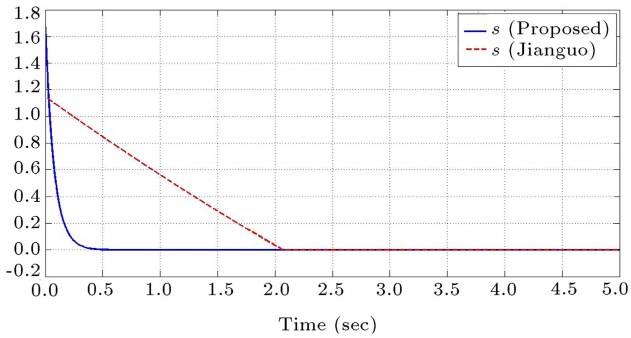

Figure 10. Response curve of the switching surface s for the proposed controller and Jianguo's controller.

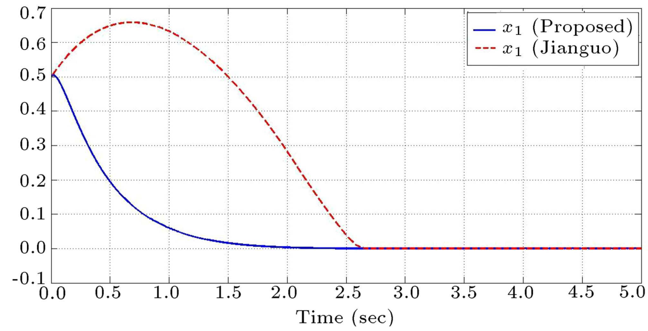

Figure 11. Response curve of x_1 for the proposed controller and Jianguo's controller.

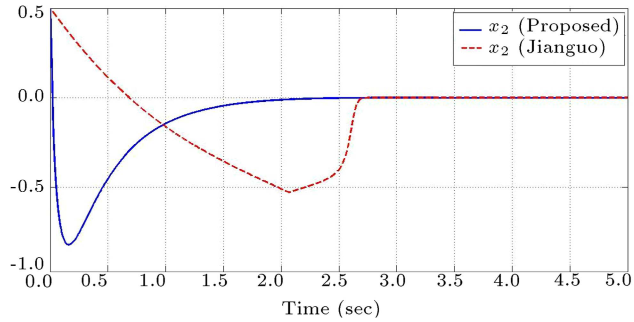

Figure 12. Response curve of x_2 for the proposed controller and Jianguo's controller.

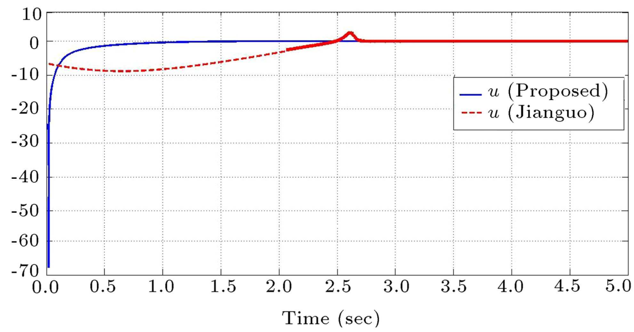

Figure 13. Response curve of the control signal u for the proposed controller and Jianguo's controller.

we applied our controller and the proposed controller of Jianguo and Shengjiang to the simulation example (SIP) without considering disturbances and reported the results of these simulations in the following.

This paper proposed the following sliding surface and control law orderly:

$$s = x_2 + \delta \frac{x_1}{|x_1| + \eta} + \gamma x_1^{\frac{m+n}{m}}, \tag{37}$$

and:

$$u = -g^{-1}(X)\left[f(X) + \frac{\delta\eta x_2}{(|x_1|+\eta)^2} + \frac{m+n}{m}\gamma x_1^{\frac{n}{m}} x_2 + k_1 s + \left(k_1 + \frac{m+n}{m}\gamma d^* |x_1|^{\frac{n}{m}}\right) sign(s)\right]. \tag{38}$$

Jianguo and Shengjian selected their parameters as follows: $\delta = 0.5$, $\eta = 0.01$, $m = 3$, $n = 2$, $\gamma = 0.5$, $k_1 = 0.1$, and $k_2 = 0.5$. Since the disturbances have not been considered, we set $d^* = 0$. Figure 10 shows the behavior of the sliding surface s. This figure indicates that the proposed controller drives the state trajectory into the sliding surface much faster than Jianguo and Shengjian's controller. This results from the fact that Jianguo and Shengjian's controller can only guarantee the finite-time stability of the reaching phase. As can clearly be understood from this figure, the sliding surface of Jianguo and Shengjian linearly converges to zero, whereas our sliding surface is driven into zero as a high-degree polynomial. The response curves of the state variables x_1 and x_2 are also depicted in Figures 11 and 12. The control signals of the two controllers are also illustrated in Figure 13. As clear from this figure, the proposed control signal is significantly larger than that of Jianguo and Shengjian. This is completely reasonable because the proposed controller stabilizes both reaching and sliding phases within fixed time whereas Jianguo and Shengjian's controller only guarantees the fixed-time stability of the sliding phase. Another remarkable feature of the proposed controller is that it generates a continuous control signal, but Jianguo and Shengjian's controller experiences chatters even when there is not any kind of disturbances (Figure 13).

5. Conclusion

This article presented a disturbance-observer-based NTSMC controller for nonlinear planar system. Its notable features included fixed-time stability of the closed-loop system, continuity of the control signal, and countering matched and mismatched disturbances. The first one guarantees the convergence time of the closed-loop system to be uniform with respect to initial conditions. The continuity of the control signal gives rise to chattering avoidance. In addition, the last one broadens the application area of the proposed controller.

6. Future recommendation

Applying the idea of the observer-based continuous FTNTSMC to the sophisticated applications such as complex dynamical networks, multi-agent systems, and so on will definitely be highly impressive and attract the attention of many researchers. Extending the proposed method to high-order planar systems can be considered a challenging problem for further research. Restructuring the proposed method in the form of output-feedback control will be also of general interest.

References

1. Jiang, T., Song, T., and Lin, D. "Integral sliding mode based control for quadrotors with disturbances: Simulations and experiments", *International Journal of Control, Automation and Systems*, **17**, pp. 1987–1998 (2019).
2. Utkin, V., Guldner, J., and Shi, J., *Sliding Mode Control in Electro-Mechanical Systems*, Boca Raton, CRC Press (2009).
3. Draženović, B. "The invariance conditions in variable structure systems", *Automatica*, **5**(3), pp. 287–295 (1969).
4. Shi, S.-L., Li, J.-X., and Fang, Y.-M. "Fractional-disturbance-observer-based sliding mode control for fractional order system with matched and mismatched disturbances", *International Journal of Control, Automation and Systems*, **17**(5), pp. 1184–1190 (2019).
5. Man, Z. and Yu, X. "Terminal sliding mode control design of mimo linear systems", *IEEE Transactions on Circuits and Systems I: Fundamental Theory and Applications*, **44**(11), pp. 823–830 (1997).
6. Feng, Y., Yu, X., and Han, F. "On nonsingular terminal sliding-mode control of nonlinear systems", *Automatica*, **49**(6), pp. 1715–1722 (2013).
7. Feng, Y., Yu, X., and Man, Z. "Non-singular terminal sliding mode control of rigid manipulators", *Automatica*, **38**, pp. 2159–2167 (2002).
8. Yang, L. and Yang, J. "Nonsingular fast terminal sliding-mode control for nonlinear dynamical systems", *International Journal of Robust and Nonlinear Control*, **21**(16), pp. 1865–1879 (2011).
9. Yong-Zhi Sheng, Jie Geng, and Xiang-Dong Liu, et al. "Nonsingular finite-time second order sliding mode attitude control for reentry vehicle", *International Journal of Control, Automation and Systems*, **13**(4), pp. 853–866 (2015).
10. Pukdeboon, C. and Siricharuanun, P. "Nonsingular terminal sliding mode based finite-time control for spacecraft attitude tracking", *International Journal of Control, Automation and Systems*, **12**(3), pp. 530–540 (2014).
11. Jun Yang, Shihua Li, Jinya Su, et al. "Continuous nonsingular terminal sliding mode control for systems withmismatched disturbances", *Automatica*, **49**, pp. 2287–2291 (2013).
12. Bhat, S. and Bernstein, D. "Finite-time stability of continuous autonomous systems", *SIAM Journal on Control and Optimization*, **38**(2), pp. 751–766 (2000).
13. Andrieu, V., Praly, L., and Astolfi, A. "Homogeneous approximation, recursive observer design, and output feedbak", *SIAM Journal on Control and Optimization*, **47**(4), pp. 1814–1850 (2008).
14. Polyakov, A. and Fridman, L. "Srtability notions and Lyapunov functions for sliding mode control systems", *Journal of Franklin Institute*, **351**(4), pp. 1831–1865 (2014).
15. Polyakov, A., Efimov, D., and Perruquetti, W. "Finite-time and fixed-time stabilization: Implicit Lyapunov function approach", *Automatica*, **51**, pp. 332–340 (2015).
16. Polyakov, A. "Nonlinear feedback design of fixed-time stabilization of linear control systems", *IEEE Transactions on Automatic Control*, **57**(8), pp. 2106–2110 (2012).
17. Zou, Z. "Non-singular fixed-time terminal sliding mode control of non-linear systems", *IET Control Theory and Applications*, **9**(4), pp. 545–552 (2014).
18. Khanzadeh, A. and Pourgholi, M. "Fixed-time leader-follower consensus tracking of second-order multi-agent systems with bounded input uncertainties using non-singular terminal sliding mode technique", *IET Control Theory and Applications*, **12**(5), pp. 679–686 (2017).
19. Fu, J. and Wang, J. "Fixed-time coordinated tracking for second-order multi-agent systems with bounded input uncertainties", *Systems & Control Letters*, **93**, pp. 1–12 (2016).
20. Zou, Z. "Nonsingular fixed-time consensus tracking for second-order multi-agent networks", *Automatica*, **54**, pp. 305–309 (2015).
21. Wei-Shun Sui, Guang-Ren Duan, Ming-Zhe Hou, et al. "Distributed fixed-time attitude synchronization control for multiple rigid spacecraft", *International Journal of Control, Automation and Systems*, **17**(5), pp. 1117–1130 (2019).
22. Corradini, M.L. and Cristofaro, A. "Nonsingular terminal sliding-mode control of nonlinear planar systems with global fixed-time stability guarantees", *Automatica*, **95**, pp. 561–565 (2018).
23. Rong Wu, Changzhu Wei, Feng Yang, et al. "Fixed-time disturbance observer based non-singular terminal sliding mode control for second-order uncertain systems", *IET Control Theory and Applications*, **12**(18), pp. 2459–2467 (2018).
24. Wen-Hua Chen, Jun Yang, Lei Guo, et al. "Disturbance-observer-based control and related methods-An overview", *IEEE Transactions on Industrial Electronics*, **63**(2), pp. 1083–1095 (2016).

25. Jun Yanga, Argyrios Zolotasb, Wen-Hua Chen, et al. "Robust control of nonlinear MAGLEV suspension system with mismatched uncertainties via DOBC approach", *ISA Transactions*, **50**(3), pp. 389–396 (2011).

26. Mohamed, Y.A.-R.I. "Design and implementation of a robust current-control scheme for a PMSM vector drive with simple adaptive disturbance observer", *IEEE Transactions on Industrial Electronics*, **54**(4), pp. 1981–1988 (2007).

27. Chang, J.-L. "Sliding mode control design for mismatched uncertain systems using output feedback", *International Journal of Control, Automation and Systems*, **14**(2), pp. 579–586 (2016).

28. Chang, J.-L. and Wu, T.-C. "Disturbance observer based output feedback controller design for systems with mismatched disturbance", *International Journal of Control, Automation and Systems*, **16**(4), p. 1775–1782 (2018).

29. Ni, J., Liu, C., and Liu, H. "Continuous uniformly finite time exact disturbance observer based control for fixed-time stabilization of nonlinear systems with mismatched disturbances", *PLoS One*, **12**(4), e0175645 (2017).

30. Angulo, M.T., Moreno, J.A., and Fridman, L. "Robust exact uniformly convergent arbitrary order differentiator", *Automatica*, **49**(8), pp. 2489–2495 (2013).

31. Shtessel, Y.B., Shkolnikov, I.A., and Levant, A. "Smooth second-order sliding modes: Missile guidance applications", *Automatica*, **43**(8), pp. 1470–1476 (2007).

32. Ming You, Qun Zong, Bailing Tian, et al. "Comprehensive design of uniform robust exact disturbance observer and fixed-time controller for reusable launch vehicles", *IET Control Theory and Applications*, **12**(5), pp. 638–648 (2017).

33. Bailing Tian, Hanchen Lu, Zongyu Zuo, et al. "Fixed-time stabilization of high-order integrator systems with mismatched disturbances", *Nonlinear Dynamics*, **94**(4), pp. 2889–2899 (2018).

34. Li, S. and Tian, Y.-P. "Finite-time stability of cascaded time-varying systems", *International Journal of Control*, **80**(4), pp. 646–657 (2007).

35. Jianguo, G. and Shengjiang, Y. "New fixed-time sliding mode control for a mismatched second-order system", *Transactions of the Institute of Measurement and Control*, **43**(2), pp. 325–334 (2020).

Biographies

Alireza Khanzadeh was born in Tehran, Iran in 1988. He received his MS from the Shahid Beheshti University in 2015 and is a PhD Candidate of Control Theory at Malek Ashtar University of Technology from 2017. His research interests include classical feedback control design with modern approaches, fixed-time stability of control systems, nonlinear control, sliding mode control, and guidance law design.

Iman Mohammadzaman is an Assistant Professor at the Faculty of Electrical and Computer Engineering, Malek Ashtar University of Technology, Tehran, Iran. His research interests include robust control, nonlinear control, and LMI optimization.